

RESEARCH ARTICLE

Platinum nanoparticles induced genotoxicity and apoptotic activity in human normal and cancer hepatic cells via oxidative stress-mediated Bax/Bcl-2 and caspase-3 expression

Mohammed H. A. Almarzoug | Daoud Ali | Saud Alarifi  | Saad Alkahtani |
Abdullah M. Alhadheq

Department of Zoology, College of Science,
King Saud University, Riyadh, Saudi Arabia

Correspondence

Daoud Ali, Department of Zoology, College of
Science, King Saud University BOX 2455,
Riyadh 11451, Saudi Arabia.
Email: dadali.ksu12@yahoo.com; aalidaoud@
ksu.edu.sa

Funding information

This research work was funded by Researchers
Supporting Project number (RSP-2019/27),
King Saud University, Riyadh, Saudi Arabia,
Grant/Award Number: This research work was
funded by Researchers Suppo

Abstract

Platinum nanoparticles (PtNPs) attract much attention due to their excellent biocompatibility and catalytic properties, but their toxic effects on normal (CHANG) and cancerous (HuH-7) human liver cells are meagre. The cytotoxic and apoptotic effects of PtNPs (average size, 3 nm) were determined in CHANG and HuH-7 cells. After treating these cells were with PtNPs (10, 50, 100, 200, and 300 µg/mL) for 24 and 48 hours, we observed dose- and time-dependent cytotoxicity, as evaluated by using (3-[4, 5-dimethylthiazol-2-yl]-2, 5-diphenyltetrazolium bromide, a tetrazole) (MTT) and neutral red uptake (NRU) assays. The production of reactive oxygen species (ROS) was increased in both cells after treatment with the above dose of PtNPs for 24 and 48 hours. Determination of morphological changes of cells, chromosome condensation, mitochondrial membrane potential, and caspase-3 assays showed that PtNPs induce cytotoxicity and apoptosis in CHANG and HuH-7 cells by altering the cell morphology and density, increasing cell population in apoptosis, and causing chromosome condensation. Furthermore, we have studied fragmentation of DNA using alkaline single cell gel electrophoresis and expression of apoptotic genes by real-time PCR (RT-PCR). The percentage of DNA fragmentation was more at 300 µg/mL for 48 hours in both cells, but slightly more fragmentation was found in HuH-7 relative to CHANG cells. Considering all of the above parameters, PtNPs elicited cytotoxicity on CHANG and HuH-7 cells by blocking cell proliferation and inducing apoptosis. Thus this study may be useful in in vitro laboratory studies using cell lines for screening the genotoxic and apoptotic potential of nanoparticles.

KEYWORDS

apoptosis, CHANG and HuH-7 cells, cytotoxicity, oxidative stress, PtNPs

1 | INTRODUCTION

Today, nanotechnology is one of the most significant technologies in science. Nanoparticles (NPs) have scales similar to biological molecules, which mean they can directly affect biological systems. Therefore, NPs are extensively applied in drug development and biomedical

health sciences.¹ Pedone et al² reported platinum NPs (PtNPs) have intrinsic catalytic properties and effectively quench the intracellular reactive oxygen species (ROS) within cells. Also, Gurunathan et al³ reported PtNPs induced apoptotic properties of doxorubicin and generation of ROS in osteosarcoma cells. Shiny et al⁴ and Yoshihisa et al⁵ reported on the use of PtNPs as synthetic enzymes in health science.

The physicochemical properties of PtNPs, such as surface area, shape, and size, control their biological activities and, ultimately affect their toxicity.⁶ All of these factors influence the delivery of NPs and their toxicological profiles, often activating unexpected apoptotic reactions and thereby increasing the contradiction of some results. The response of the apoptotic system to PtNPs has been poorly investigated. Here we investigate the toxicity of PtNPs on normal and cancerous human liver cell lines.

NPs are internalized into different organelles of exposed cells in a pH-dependent manner. Paraskar et al⁷ suggested that NPs could be used as antitumour agents in a 4 T1 breast cancer model. Apoptosis, autophagy, necroptosis, aponecrosis, pyroptosis, and necrosis are major cell death mechanisms.⁸ Ksiazek et al⁹ reported the toxic effects of silver and platinum NPs on the freshwater microalga *Pseudokirchneriella subcapitata*. It has been hypothesized that NPs disorder and impair cell functions via multiple mechanisms.¹⁰ NPs have some ions or toxic materials that indirectly or directly affect living cells via the production of ROS. Some researchers reported that cell toxicity occurs due to ROS-generating environmental pollutants and NPs.^{11,12} Verma et al¹³ reported that NPs cross or adhere to biological membranes and induce cellular damage.

The generation of more ROS provokes fragmentation of nuclear molecules, damage to the cellular macromolecules, and apoptosis. Thus, in this study, we evaluated the toxic and apoptotic potential of PtNPs on normal and cancerous human liver cells.

2 | MATERIALS AND METHODS

2.1 | Chemical and reagents

Platinum NPs (PtNPs, average particle size <3 nm particle size, stock #:7801) were purchased from US Research Nanomaterials, Inc. Antibiotic antimycotic solution (cat no. A5955) (Sigma-Aldrich Chemie GmbH, Taufkirchen, Germany), MTT (1-[4,5-dimethylthiazol-2-yl]-3,5-diphenylformazan, thiazolyl blue formazan), Neutral red dye (NRU), 5,5'-dithiobis(2-nitrobenzoic acid) (DTNB), 2',7'-dichlorodihydrofluorescein diacetate (H2DCFDA), dimethyl sulfoxide (DMSO), Annexin V, FITC, and propidium iodide (PI) were obtained from Sigma-Aldrich. Culture media (DMEM), fetal bovine serum (FBS), and antibiotics were bought from Gibco (Manassas, Virginia 20110).

2.2 | Cell culture

Human normal (CHANG) and cancer (HuH-7) liver cells were purchased from American Type Culture Collection (ATCC) (Manassas, Virginia 20110). CHANG and HuH-7 cells were grown in culture medium containing FBS (10%) and antibiotic-antimycotic solution (10 000 U/mL, [1%]) in a CO₂ (5%) incubator at 37°C. After reaching 80% confluence, cells were recultured into 96-well plates, 6-well plates, or 25 cm² flasks according to our experiments.

2.3 | Exposure to PtNPs

CHANG and HuH-7 cells were grown for 24 hours before treating with PtNPs. A suspension (1 mg/mL) of PtNPs was prepared in culture medium and diluted to our experimental concentrations (10, 50, 100, 200, and 300 µg/mL). NP dispersion was done using a sonicator (Qsonica 500 New York) at 40 kHz for 15 minutes at room temperature before proceeding to exposure. The control cells were not exposed to PtNPs.

2.4 | Physical characterization of PtNPs

2.4.1 | Transmission electron microscopy (TEM)

An original suspension of PtNPs (1 mg/mL) was made in double-distilled water. The carbon-coated copper grid was dipped into the suspension of the highest dose of PtNPs (300 µg/mL) solution and was dried for 24 hours. After drying the grid, the photomicrograph of NPs was taken using a TEM (JEOL Inc., Tokyo, Japan) at 120 kV. We have counted 20 areas of the TEM grid.

2.4.2 | Dynamic light scattering (DLS)

The hydrodynamic size and zeta potential of PtNPs in water suspension were measured using dynamical light scattering (DLS, Nano-Zeta Sizer-HT, Malvern, UK), as described by Alarifi et al method.¹⁴ The PtNPs powder (300 µg) was mixed in per mL of double distilled water and the culture media and sonicated at 40 W for 10 minutes by sonicator (Qsonica 500 New York).

2.5 | Morphological study of CHANG and HuH-7 cells

The cells were exposed to different concentrations of NPs (10, 50, 100, 200, and 300 µg/mL) for 48 hours. The effects of PtNPs on the morphology of CHANG and HuH-7 cells were assessed under an inverted phase-contrast microscope (Nikon Eclipse Ti-S Japan).

2.6 | MTT assay

The cytotoxic effect of PtNPs (10, 50, 100, 200, and 300 µg/mL) on both cell types were determined using the MTT assay, as described by AlKahtane et al method.¹⁵ Briefly, 1×10^4 cells/well were plated in a culture plate (96 well) and exposed to PtNPs for 48 hours. The media was discarded from the 96-well plates, and 100 µL MTT (5 mg/mL) solution per well was added and incubated for 4 hours at 37°C. After incubation, the culture plates were rinsed with cold phosphate buffer saline (PBS) and formazan crystal dissolved in dimethylsulphoxide, and

the optical density (OD) was measured at 570 nm using a microplate reader (Synergy-HT; BioTek, Winooski, Vermont).

2.7 | NRU test

The NRU test was done according to the Borenfreund and Puerner¹⁶ method to confirm the toxic effect of PtNPs (10, 50, 100, 200, and 300 µg/mL) on both cell types. After exposure to PtNPs, the cells were cleaned with chilled saline buffer, and neutral red dye was added (100 µL with DMEM for 4 hours), and after

incubation, the cells were washed with fixative and simultaneously dye extractor solution. The OD was taken at 540 nm using a spectrophotometer.

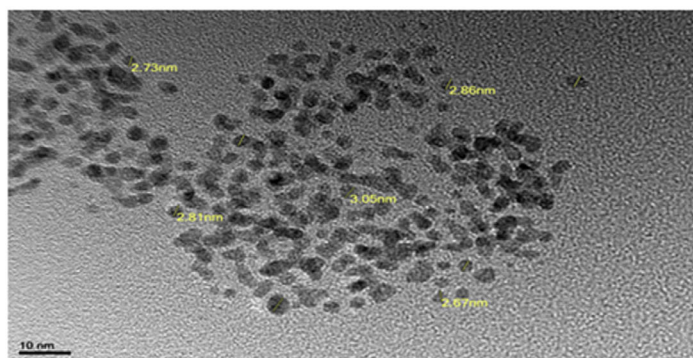
2.8 | Reactive oxygen species

The generation of ROS in both cells due to PtNPs (10, 50, 100, 200, and 300 µg/mL) was done using H2DCFDA according to methods described by Almeer et al.¹⁷ Both cells were cultured (2×10^4 cells/well) in 96-well black plates for 20 hours and then

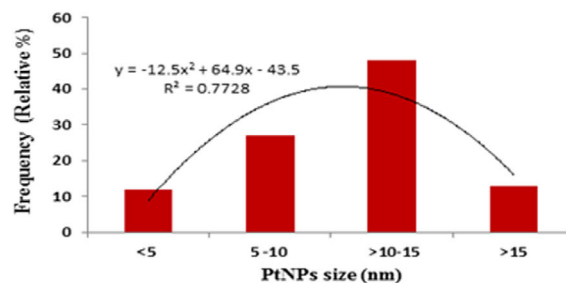
TABLE 1 List of primer with sequences

Genes	Primer sequences (5' to 3')	Gen bank accession number	PCR product size (bp)
Bax	F-5'-ATGTTTTCTGACGGCAACTTC-3' R-5'-AGTCCAATGTCCAGCCCAT-3'	NM_004324	133
Bcl-2	F-5'-ATGTGTGTGGAGACCGTCAA-3' R-5'-GCCGTACAGTTCACAAAGG-3'	NM_000633	141
Caspase-3	F-5'-TGTTTGTGTGCTTCTGAGCC-3' R-5'-CACGCCATGTCATCATCAAC-3'	NC_000004.12	210
GAPDH	F-5'-GACTTCAACAGCGACACCCACTCC-3' R-5'-AGGTCACCACCTGTTGCTGTAG-3'	NM_002046	125

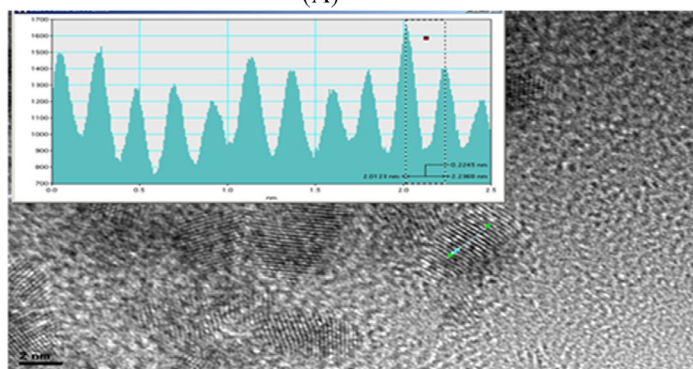
Abbreviations: F, forward; R, reverse.



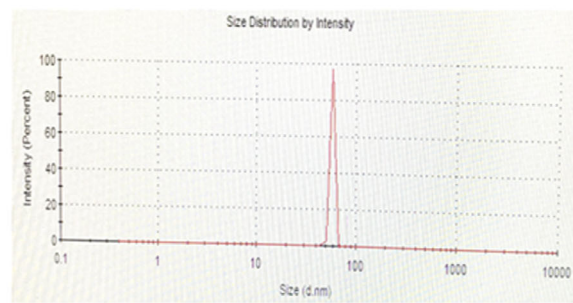
(A)



(B)



(C)



(D)

FIGURE 1 A, The image of platinum nanoparticles taken by transmission electron microscopy (JEOL Inc. Tokyo, Japan). B, Percentage frequency of size of platinum nanoparticles distribution. C, Distance among two platinum nanoparticles. D, Hydrodynamic size of platinum nanoparticles [Color figure can be viewed at wileyonlinelibrary.com]

treated with NPs for 24 and 48 hours. H2DCFDA (20 μ M) was added to the cells for 30 minutes. After incubation, the culture plate was washed with chilled PBS and the fluorescence of dichlorofluorescein was evaluated using a plate reader (Spectra MAX Gemini EM, Molecular Devices) at 480 nm excitation and 530 nm emissions.

For qualitative analysis of ROS generation in both cells due to NPs, we have simultaneously set-up another experiment in a 6-well transparent plate (1×10^3 cells/well) and intracellular ROS generation was monitored using a fluorescent microscope (Olympus CKX41; Olympus: Center Valley, Pennsylvania), with images taken at $\times 10$ magnification.

2.9 | Cell lysate

PtNPs (10, 50, 100, 200, and 300 μ g/mL) exposed and nonexposed CHANG and HuH-7 cells were rinsed with PBS and collected in an Eppendorf tube through scraping. Lysis buffer was mixed in scrapped cells and centrifuged at 13 000 rpm for 15 minutes at 4°C, and the supernatant (cell lysate) was put on ice for further tests for reduced glutathione (GSH), lipid peroxide (LPO), and catalase.

The quantity of total protein in the cell lysate was evaluated by the Bradford method¹⁸ using bovine serum albumin as the standard.

2.9.1 | GSH test

The GSH content was evaluated according to Ellman's method.¹⁹ Cell lysate (100 μ L) was added to trichloroacetic acid (TCA) (5%, TCA 900 μ L) and centrifuged at 3000g for 10 minutes at 4°C. Again, 500 μ L of supernatant was added to DTNB (0.01%, 1.5 mL), and the OD of the mixture was observed at 412 nm. The quantity of GSH was represented as a n mole/mg protein.

2.9.2 | LPO test

LPO was measured according to the Ohkawa et al method.²⁰ Briefly, 1.9 mL PBS (0.1 M, pH 7.4) was added to 100 μ L cell lysate and left at 37°C for 60 minutes. After 60 minutes, TCA (5%) was added, and the mixture centrifuged at 3000 rpm for 15 minutes at room temperature. The supernatant was mixed with thiobarbituric acid (1%, 1 mL) and incubated in a water bath at 100°C for 30 minutes. A pink color developed and the OD was measured at 532 nm and expressed as n mol MDA/mg protein.

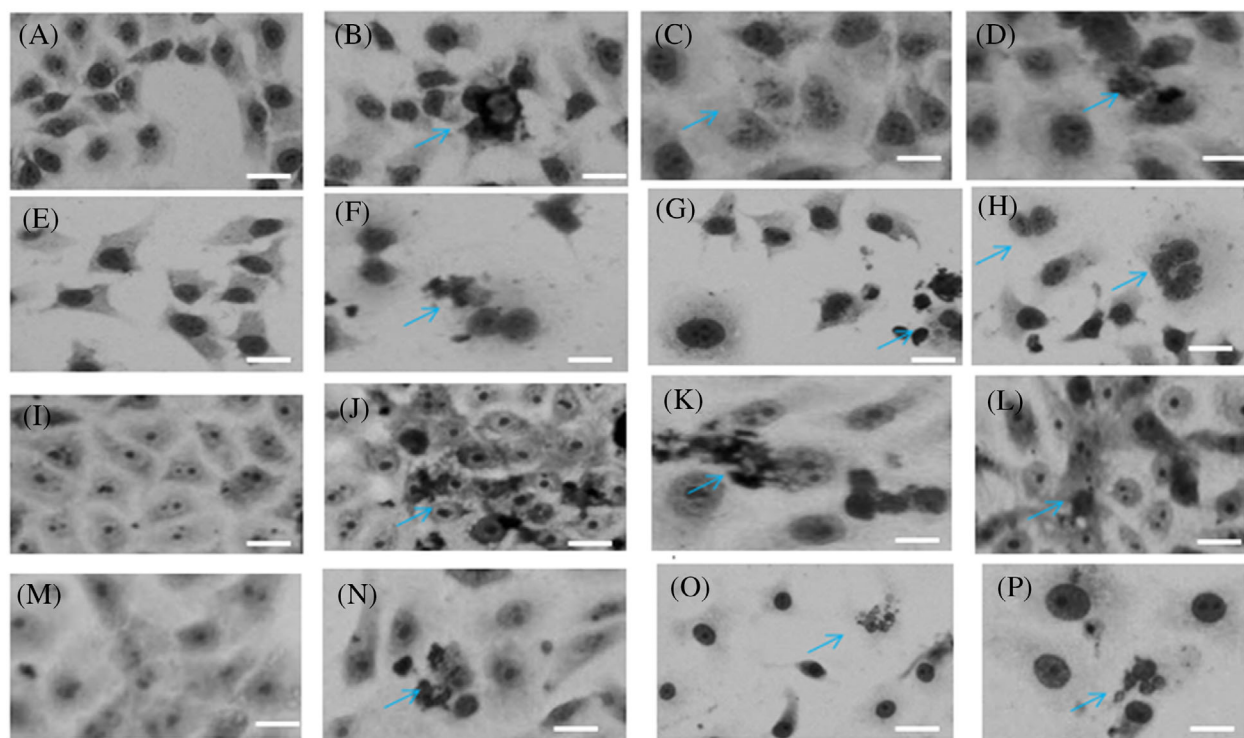


FIGURE 2 Morphological changes in CHANG and HuH-7 cells exposed to different concentrations of PtNPs for 24 ad 48 hours. A, Control CHANG cells in 24 hours. B, CHANG cells at 50 μ g/mL in 24 hours. C, CHANG cells at 200 μ g/mL in 24 hours. D, CHANG cells at 300 μ g/mL in 24 hours. E, Control CHANG cells in 48 hours. F, CHANG cells at 50 μ g/mL in 48 hours. G, CHANG cells at 200 μ g/mL in 48 hours. H, CHANG cells at 300 μ g/mL in 48 hours. I, Control HuH-7 cells in 24 hours. J, HuH-7 cells at 50 μ g/mL in 24 hours. K, HuH-7 cells at 200 μ g/mL in 24 hours. L, HuH-7 cells at 300 μ g/mL in 24 hours. M, Control HuH-7 cells in 48 hours. N, HuH-7 cells at 50 μ g/mL in 48 hours. O, HuH-7 cells at 200 μ g/mL in 48 hours. P, HuH-7 cells at 300 μ g/mL in 48 hours. Scale bars are 100 μ m. Arrow indicates damaged cells [Color figure can be viewed at wileyonlinelibrary.com]

2.9.3 | Catalase

Catalase was evaluated in both cells using Cayman chemical kits (Item no. 707002) according to the manufacturer's instructions. The quantity of catalase was represented as a Unit/mg protein.

2.10 | Mitochondrial membrane potential (MMP)

JC-1 fluorescent staining was used to detect the level of change in the MMP of CHANG and HuH-7 cells. The cells were exposed to the PtNPs (200 and 300 $\mu\text{g}/\text{mL}$) for 24 and 48 hours. After exposure for the specified duration, the cells were rinsed, and JC-1 (5 μM , Cayman chemical) was added for 30 minutes at 37°C. A parallel experiment was carried out to determine the J-aggregate and J-monomer ratios. Both cell lines were seeded in a black 96-well plate and incubated with different concentrations of PtNPs (10, 50, 100, 200, or 300 $\mu\text{g}/\text{mL}$) for 24 and 48 hours. After incubation, the fluorescence of the J-aggregates and J-monomers was evaluated using a fluorescence microplate reader (Spectra MAX Gemini EM, Molecular Devices) at 530/590 nm (excitation wavelength/

emission wavelength) for the J-aggregates and 480/528 nm (excitation wavelength/emission wavelength) for the J-monomers.

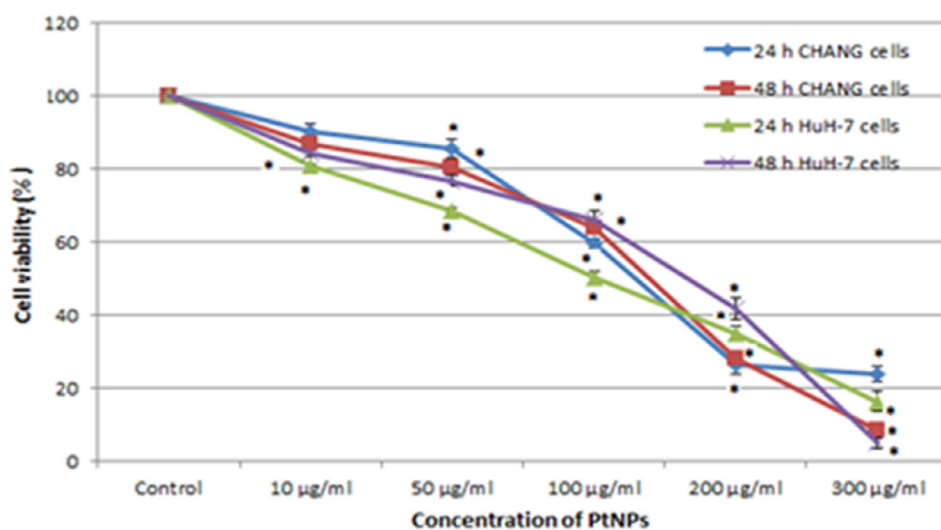
2.11 | Evaluation of caspase-3 activity and chromosome condensation

The effect of PtNPs (10, 50, 100, 200, or 300 $\mu\text{g}/\text{mL}$) on the caspase-3 activity in CHANG and HuH-7 cells were evaluated using a colorimetric kit (Cayman Chemical) according to the manufacturer's instructions.

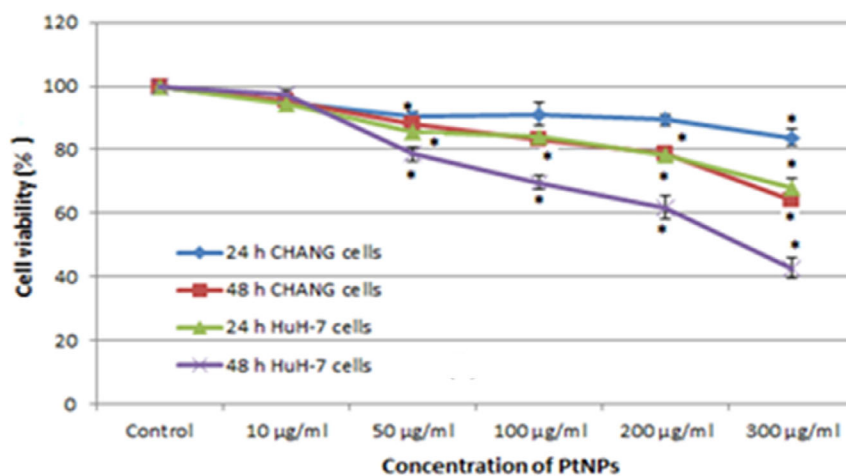
The condensation of the chromosomes after treatment with PtNPs (200 or 300 $\mu\text{g}/\text{mL}$) for 24 and 48 hours in both cell lines was observed by Hoechst 33342 staining. Fragmented chromosomes were observed in both of the treated cell lines according to the method described in Alarifi et al.²¹

2.12 | Alkaline single-cell gel electrophoresis

DNA damage in both CHANG and HuH-7 cells was determined using a single-cell gel test, according to Ali et al.²² After electrophoresis, the slide



(A)



(B)

FIGURE 3 Cytotoxicity of platinum nanoparticles on CHANG and HuH-7 cells for 24 and 48 hours as determined by A, MTT tests and B, NRU tests. Each value represents the mean \pm SE of three experiments. $n = 3$, * $P < .05$ vs control. Arrow indicates high generation of intracellular ROS in cells [Color figure can be viewed at wileyonlinelibrary.com]

was rinsed with neutralization buffer and stained with ethidium bromide. We have screened 50 random cells (25 from each replicate slide) for each experiment. Single-strand breakage was determined as the proportion of tail DNA and the olive tail moment (OTM) using the Komet software.

2.13 | RNA isolation, cDNA synthesis, and RNA analysis

RNA was isolated using an *RNeasy Mini Kit* (Cat No. /ID: 74104). The purity and concentration of RNA were measured using a Nanodrop (DS-11; Bio-Rad Laboratories Inc., Hercules, California). The purity of RNA (A260/A280 ratio) sample was ~2. We have synthesized cDNA from RNA (250 ng) using a cDNA reverse transcription kit (Revert Aid First Strand cDNA Synthesis Kit; Thermo Fisher Scientific). Analysis of Bax, Bcl-2, and caspase-3 mRNA levels was done by RT-PCR (PE Applied Biosystems, Foster City, California). The primer sequences targeting apoptotic genes are listed in Table 1. The RT-PCR parameters were: 5 minutes at 95°C for initial denaturing, followed by 30 cycles, 10 seconds at 95°C, and 1 minute at 50°C. The cycle

threshold (Ct) values were standardized to the housekeeping gene (*GAPDH*), and data were analyzed using the comparative the $\Delta\Delta C_t$ method²³ and the expression of target genes was normalized to *GAPDH*. Each experiment was performed with three replicates.

2.14 | Statistical analysis

The present data were analyzed by one-way analysis of variance (ANOVA), and the significant value was set at $P < .05$.

3 | RESULTS

3.1 | Characterization of PtNPs

The size, surface area, and structure of NPs were examined by high-resolution transmission electron microscope (HR-TEM) and DLS methods. We have counted 100 separate NPs for size determination. The average size of 100 PtNPs was 6.30 ± 2.4 nm. Figure 1A shows a

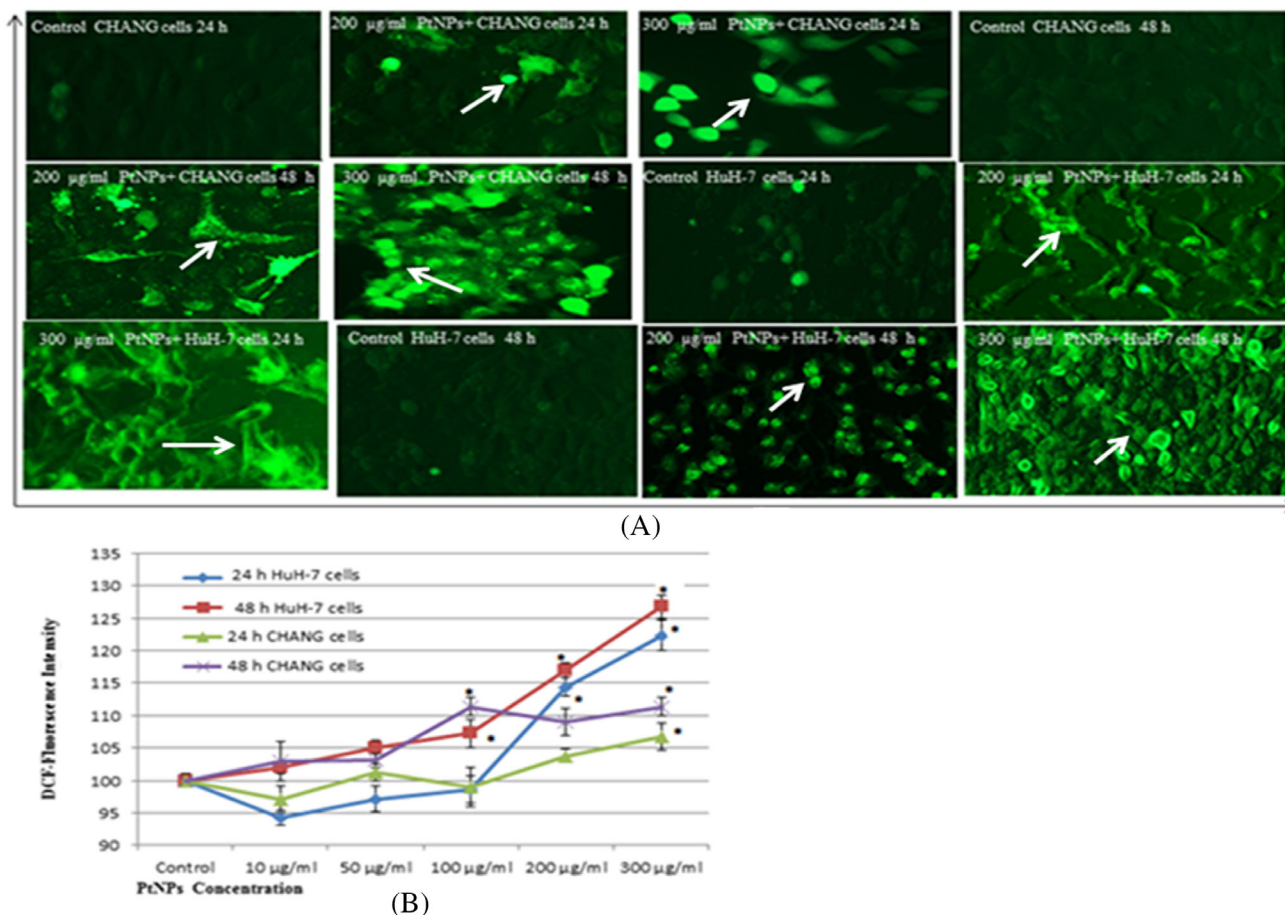


FIGURE 4 Intracellular ROS generation after exposure to PtNPs. A, The fluorescence image CHANG and HuH-7 cells treated with 200 µg/mL and 300 µg/mL nanoparticles for 24 and 48 hours and stained with DCFHDA. B, %ROS production due to platinum nanoparticle in image CHANG and HuH-7 cells. Each value represents the mean \pm SE of three experiments. * $P < .05$ [Color figure can be viewed at wileyonlinelibrary.com]

TEM image of the PtNPs. The average size frequency (%) of the PtNPs is presented in Figure 1B. Figure 1C shows the distance among two platinum NPs in suspension. The hydrodynamic size of PtNPs was 58.53 nm, and the zeta potential was -8.6 mV.

3.2 | Morphology of CHANG and HuH-7 cells

After exposure to PtNPs, the morphology of CHANG and HuH-7 cells were changed, and most of the cells became fragmented and spherical and left the surface of the culture flask in a dose- and time-dependent manner (Figure 2).

3.3 | Cell viability

The cell viability of CHANG and HuH-7 cells after exposure to PtNPs was determined by MTT and NRU assays. We have found 90.45%, 85.71%, 59.52%, 26.19%, and 23.91% in 24 hours and 86.71%, 80.42%, 63.60%, 27.90%, and 8.31% in 48 hours cell viability of CHANG cells after exposure of different concentration of PtNPs (Figure 3A). Also, the results of cell viability were 81.0%, 68.62%, 50.2%, 34.68%, and 16.24% in 24 hours and 84.32%, 76.73%, 65.79%, 41.52%, and 4.78% in 48 hours for HuH-7 cells (Figure 3A). We have observed that the cytotoxic effects of PtNPs on both cell

types are dose- and time-dependent. The findings of the NRU assay were in line with the MTT assay results (Figure 3B).

3.4 | ROS generation activity and oxidative stress

PtNPs induced intracellular ROS in both cells in a time- and dose-dependent manner (Figure 4A,B). The maximum production of intracellular ROS was +168% (relative to the control) in CHANG cells at 300 $\mu\text{g}/\text{mL}$ PtNPs for 48 hours. It is noteworthy that PtNPs induced more intracellular ROS generation in CHANG cells than HuH-7 cells (Figure 4A,B).

The CHANG and HuH-7 cells showed a higher intensity of dichlorofluorescein (as green fluorescence, a marker of intracellular ROS generation) compared to the control when exposed to 300 $\mu\text{g}/\text{mL}$ PtNPs for 48 hours (Figure 4B).

Nita and Grzybowski²⁴ reported that mitochondrial DNA molecules were broken and repaired by ROS. The ratio of MDA, which is a target product of LPO, was significantly increased, but GSH and catalase levels were reduced at a higher dose of PtNPs (300 $\mu\text{g}/\text{mL}$) for 48 hours (Figure 5A-C).

3.5 | Determination of MMP

Loss of MMP in CHANG and HuH-7 cells was measured using the JC-1 staining method, and the maximum loss of MMP was recorded

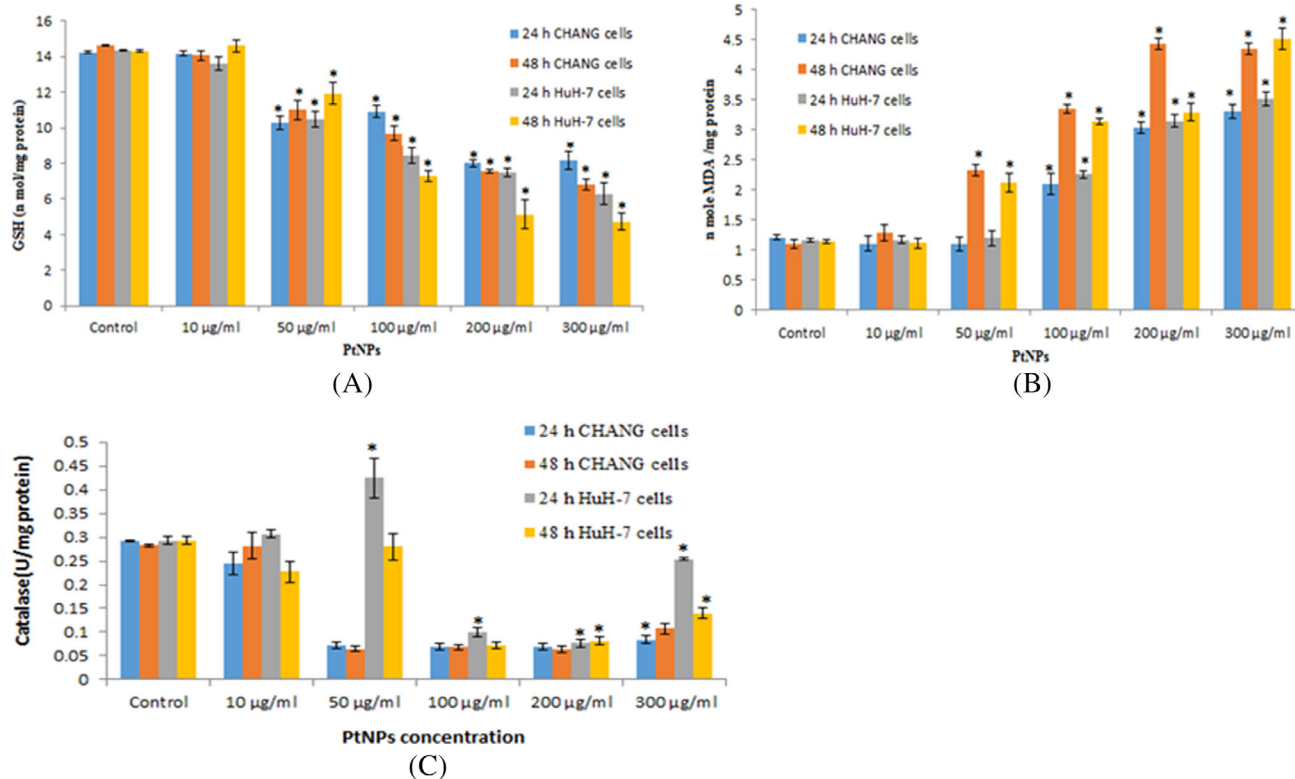


FIGURE 5 A, Percentage increase of GSH. B, percentage increase of LPO. C, level of catalase after exposure to platinum nanoparticles for 24 hours and 48 hours. Each value represents the mean \pm SE of three experiments. * $P < .05$ vs control [Color figure can be viewed at wileyonlinelibrary.com]

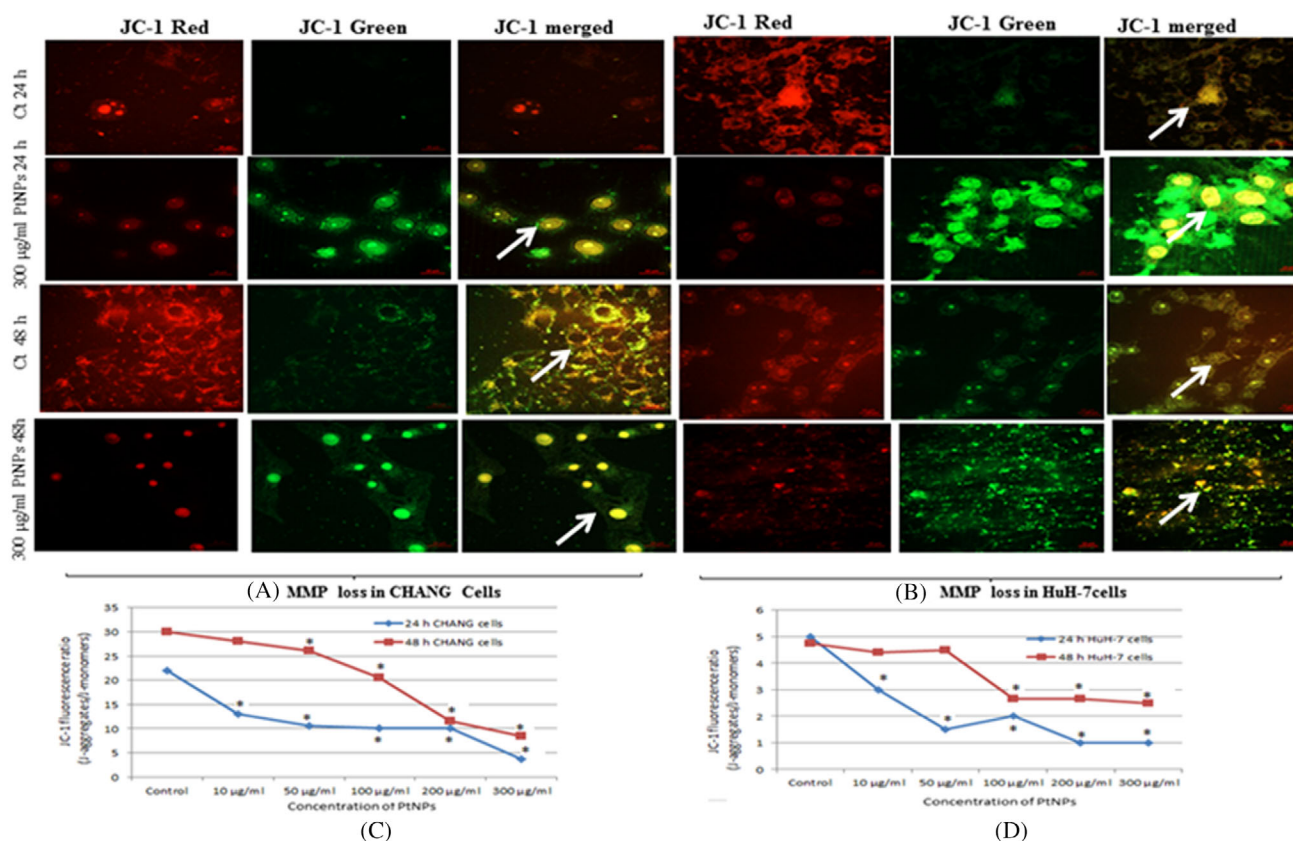


FIGURE 6 Images representing MMP loss in CHANG and HuH-7 cells after platinum nanoparticles exposure at concentration of 300 µg/mL for 24 and 48 hours. A, MMP loss in CHANG cells. B, MMP loss in HuH-7 cells. C, Change in MMP in CHANG cells. D, Change in MMP in HuH-7 cells. Each value represents the mean \pm SE of three experiments. * $P < .05$ vs control. Arrow indicates loss of MMP in cells [Color figure can be viewed at wileyonlinelibrary.com]

at a higher concentration of PtNPs. Hirsch et al²⁵ have reported that the mitochondrial permeability of apoptotic and necrotic cells is compromised due to oxidative stress. The strong MMP was found in both control cells as JC-1 dye penetrate to cells and produced J-aggregates, with deep red fluorescence. But both cells at 300 µg/mL PtNPs exposure decreased their MMP and did not incorporate JC-1 stain (Figure 6A-D).

3.6 | Chromosome condensation and caspase-3 level

After treatment with PtNPs, the apoptotic and necrotic effects of NPs on both cells were observed using chromosome condensation and caspase-3 activities. The nucleus of control cells remained intact and emitted blue fluorescence, whereas cells exposed to PtNPs had fragmented nuclear materials with intense blue fluorescence (Figure 7A).

The activity of caspase-3 (trademark of apoptosis) is increased in NP-treated cells compared to the control (Figure 7B,C). Caspase-3

activity was increased (in a dose-dependent manner) in CHANG and HuH-7 cells due to PtNPs treatment (Figure 7B,C).

3.7 | DNA damage

DNA fragmentation due to treatment with PtNPs in both cells was determined using the comet test. The cells showed more DNA damage as the PtNPs concentration and time of treatment were increased (Figure 8). In CHANG and HuH-7 cells exposed to PtNPs, the DNA tail length was 33 µm longer than in the control.

3.8 | Expression of apoptotic genes

We have screened some apoptosis-related genes (*Bax*, *Bcl2*, and *caspase-3*) by RT-PCR. The preapoptotic *Bax* gene was up-regulated in CHANG cells in 24 hours (Figure 9A) and was up-regulated in 24 hours for HuH-cells and 48 hours for CHANG and HuH-7 cells (Figure 9B-D). However, *Bcl2* was significantly down-regulated at all

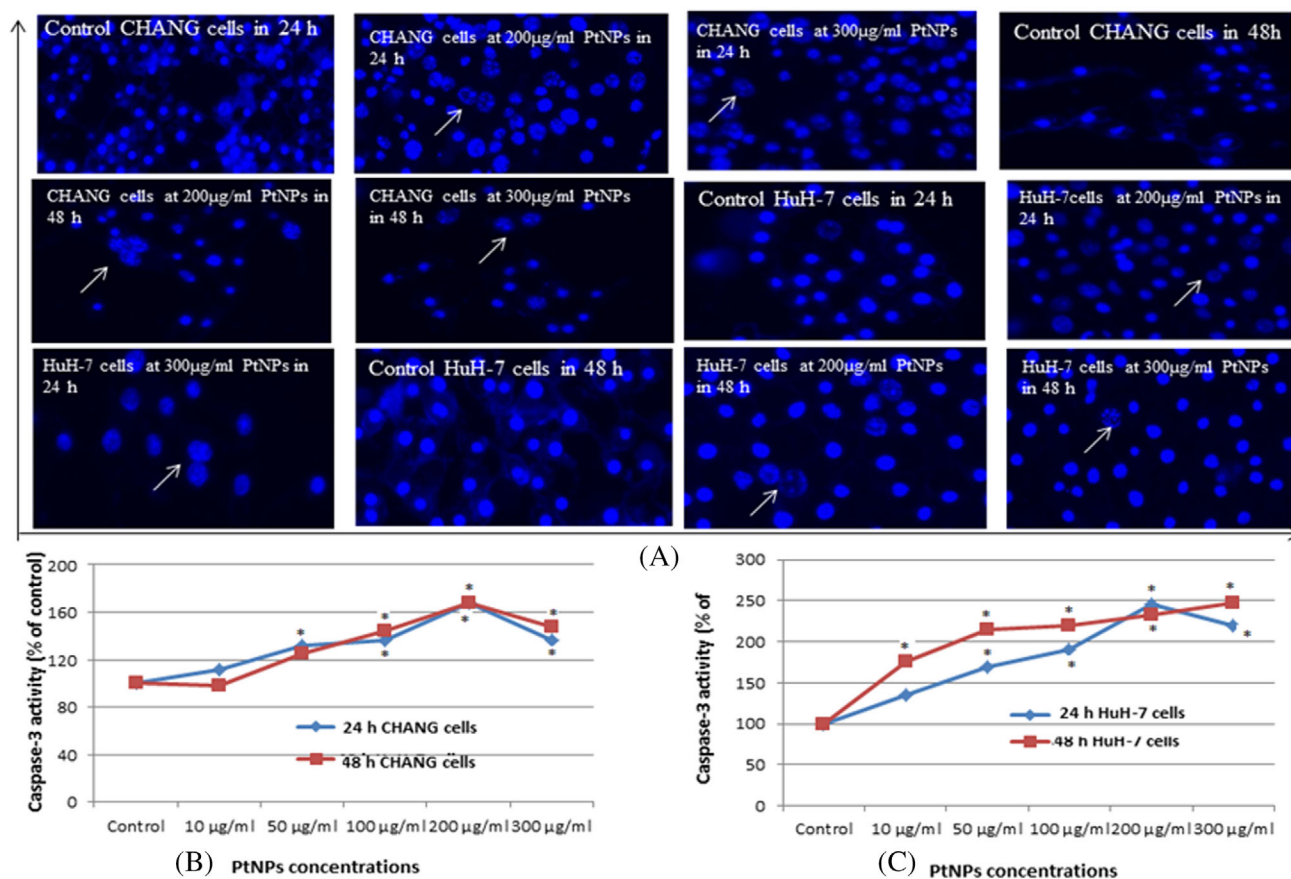


FIGURE 7 A, Chromosomal condensation and B, Induction of caspase-3 activity in CHANG cells after exposure to platinum nanoparticles for 24 hours and 48 hours C, Induction of caspase-3 activity in HUH-7 cells after exposure to platinum nanoparticles for 24 hours and 48 hours. Each value represents the mean \pm SE of three experiments. * $P < 0.05$ vs control [Color figure can be viewed at wileyonlinelibrary.com]

concentrations and time points except at 100 $\mu\text{g}/\text{mL}$ for 48 hours (Figure 9A-D). The *caspase 3* gene was up-regulated after exposure to PtNPs for 24 and 48 hours (Figure 9A-D).

4 | DISCUSSION

Currently, nanotechnology is a broad field of science and is more beneficial to human life. Since nanosized particles are more biocompatible than conservative therapeutic agents, an important research goal is to improve the bioavailability and biocompatibility of NPs for therapeutic applications in diseases such as cancer.²⁶ Therefore, in this study, we evaluated the cytotoxicity and apoptotic effects of platinum NPs (PtNPs) using normal and cancerous liver cell lines to determine their toxicity under in vitro conditions. In this experiment, we used 3-nm PtNPs (as reported by the supplier); however, after being suspended in culture media, the resulting size of the PtNPs was larger than its original size as determined by TEM and DLS. The mean particle sizes and size distribution of the NPs (measured by DLS) were enhanced when measured in aqueous media compared to measurements in the dry phase (by TEM). Krishnamoorthy²⁷ and Petosa et al,²⁸ reported that NPs—due to their high specific surface area and high surface

energy have the propensity to aggregate together to form micro-sized particles that are more stable in the environment.

In this study, we observed that PtNPs are more effective in HuH-7 cells than in CHANG cells. We found that PtNPs induced more cell death in HuH-7 cells. In contrast, a small cytotoxic effect was observed in normal liver cells with PtNPs at a concentration of 300 $\mu\text{g}/\text{mL}$, suggesting that the cytotoxic effect on the liver cancer cell line was due to the PtNPs. PtNPs induced greater cytotoxicity in the HuH-7 cell line, and thus, the HuH-7 cell line was selected to determine the mode of action and anticancer potential of the PtNPs.

The biosafety and biocompatibility of any biomaterial are vital concerns that should be addressed before the biomaterials are applied to biological systems. Mironava et al²⁹ reported that platinum folate NPs are more cytotoxic to cancerous keratinocytes SCC12B and SCC13 than to normal keratinocytes, the normal breast cell line MCF10A and the cancerous breast cell line MCF7. Thus, the findings of this study were consistent with the findings of Mironava et al.²⁹ Bendale et al³⁰ reported that PtNPs (100 $\mu\text{g}/\text{mL}$) did not induce toxic effects in normal peripheral blood mononucleocytes.

We measured the cytotoxic effect of PtNPs in CHANG and HuH-7 cells by applying the MTT and NRU tests. The free radicals that are produced intracellularly affect cell organelles and cellular

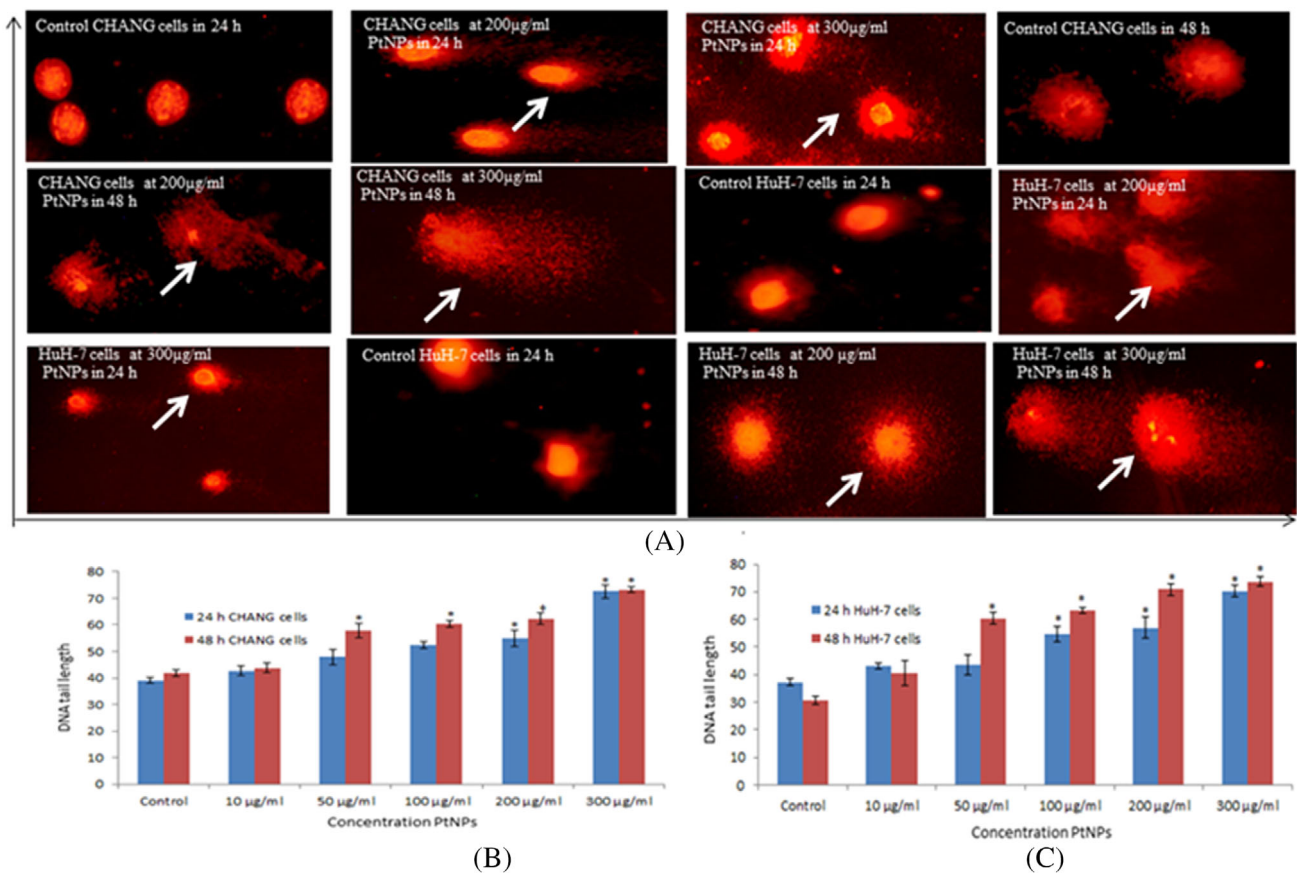


FIGURE 8 A, Photomicrograph of DNA damage in CHANG and HuH-7 cells. B, DNA damage and DNA tail length in CHANG cells after exposure to platinum nanoparticles for 24 and 48 hours. C, Induction of DNA tail length in HuH-7 cells for 24 and 48 hours. Each value represents the mean \pm SE of three experiments [Color figure can be viewed at wileyonlinelibrary.com]

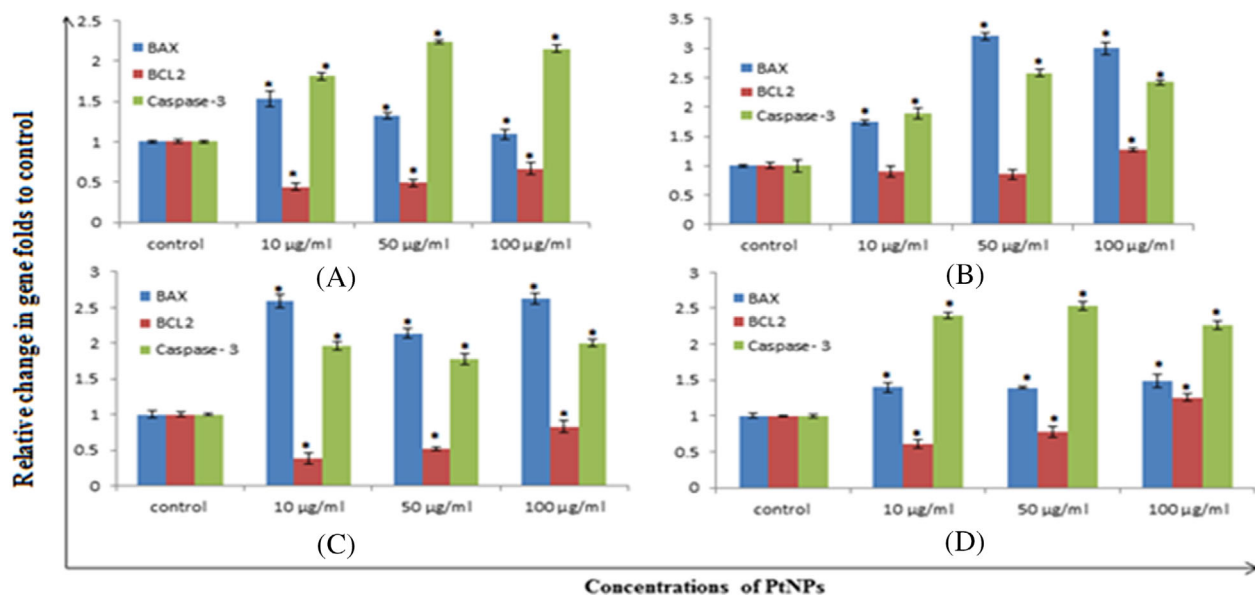


FIGURE 9 Quantitative real time PCR analysis of expression of apoptotic genes in CHANG and HuH-7 cells exposed to platinum nanoparticles for 24 hours and the expression of: A, Expression of Bax, Bcl-2, and caspase-3 gene in CHANG cells in 24 hours. B, Expression of Bax, Bcl-2, and caspase-3 gene in CHANG cells in 48 hours. C, Expression of Bax, Bcl-2, and caspase-3 gene in HuH-7 cells 24 hours. D, Expression of Bax, Bcl-2, and caspase-3 gene in HuH-7 cells in 48 hours. Results are expressed as average \pm SE of triplicate experiments. * $P < .05$ vs control [Color figure can be viewed at wileyonlinelibrary.com]

substances, such as carbohydrates, fats, proteins, and DNA molecules.³¹ PtNPs increased caspase-3 activity and the number of fragmented chromatin in these cells.

However, PtNPs cause intracellular ROS production, which results in oxidative damage and apoptosis.³² In both cell lines, PtNPs generated ROS, decreased GSH, increased lipid peroxides, and damaged DNA, which led to damage to the cellular components of the cells. To determine the mechanism behind PtNPs-induced cell death, we examined the alterations of different biomarkers involved in apoptosis. Susin et al³³ suggested that mitochondria plays an important role in apoptosis and that the disintegration of mitochondrial integrity might be prevented by various biomarkers of apoptosis. Oxidative stress leads to the activation of caspase enzymes in the cytoplasm via the involvement of cytochrome-c in the intermembrane space.³⁴

We have observed that cell toxicity after treatment with PtNPs in both cell lines occurs through apoptosis and necrosis. Our results are in line with the finding of Almeer et al¹⁷ using green platinum NPs for human embryonic kidney cells. The sensitivity of different cells to NP exposure has been reported by many researchers.^{35,36} It is well established that necrosis is usually related to the loss of lysosomal membrane integrity,³⁷ while apoptosis is caused by caspase activation, calcium overload, or death-inducing signals.^{38,39} Therefore, the mechanism of PtNPs and the subsequent cytotoxic process in this experiment seems to be cell line specific. This result might be further employed for anticancer drug formulations.

5 | CONCLUSION

Based on the above findings, we conclude that PtNPs induced cytotoxic and apoptotic activity against normal and cancerous liver cells but that the cancerous cells are more susceptible to the PtNP effects than normal cells. Based on our observations, we suggest that PtNPs represent an emerging novel therapeutic agent for the treatment of human liver cancer with little cytotoxicity towards normal cells. Further studies are needed to support our observations of the antitumor potential of these platinum NPs in vivo.

ACKNOWLEDGEMENT

This research work was funded by Researchers Supporting Project number (RSP-2019/27), King Saud University, Riyadh, Saudi Arabia.

CONFLICT OF INTERESTS

The authors declare no potential conflict of interest.

ORCID

Saud Alarifi  <https://orcid.org/0000-0001-9824-5089>

REFERENCES

- Mura S, Nicolas J, Couvreur P. Stimuli-responsive nano-carriers for drug delivery. *Nat Mater*. 2013;12:991-1003.
- Pedone D, Moglianetti M, De Luca E, Bardi G, Pompa PP. Platinum nanoparticles in nanobiomedicine. *Chem Soc Rev*. 2017;46:4951-4975.
- Gurunathan S, Jeyaraj M, Kang MH, Kim JH. Tangeretin-assisted platinum nanoparticles enhance the apoptotic properties of doxorubicin: combination therapy for osteosarcoma treatment. *Nanomaterials*. 2019;9:1089.
- Shiny PJ, Mukherjee A, Chandrasekaran N. Haemocompatibility assessment of synthesized platinum nanoparticles and its implication in biology. *Bioprocess Biosyst Eng*. 2014;37:991-997.
- Yoshihisa Y, Zhao QL, Hassan MA, et al. SOD/catalase mimetic platinum nanoparticles inhibit heat-induced apoptosis in human lymphoma U937 and HH cells. *Free Radic Res*. 2011;45:326-335.
- Albanese A, Tang PS, Chan WCW. The effect of nanoparticle size, shape, and surface chemistry on biological systems. *Annu Rev Biomed Eng*. 2012;14:1-16.
- Paraskar A, Soni S, Basu S, et al. Rationally engineered polymeric cisplatin nanoparticles for improved antitumor efficacy. *Nanotechnology*. 2011;22(26):1-13.
- Bergsbaken T, Fink S, Cookson BT. Pyroptosis: host cell death and inflammation. *Nat Rev Microbiol*. 2009;7:99-109.
- Książczyk M, Asztemborska M, Stęborowski R, Bystrzejewska-Piotrowska G. Toxic effect of silver and platinum nanoparticles toward the freshwater microalga *Pseudokirchneriella subcapitata*. *Bull Environ Contam Toxicol*. 2015;94:554-558.
- Huang YW, Cambre M, Lee HJ. The toxicity of nanoparticles depends on multiple molecular and physicochemical mechanisms. *Int J Mol Sci*. 2017;18:2702.
- Moosavi MA, Sharifi M, Ghafary SM, et al. Photodynamic N-TiO₂ nanoparticle treatment induces controlled ROS-mediated autophagy and terminal differentiation of leukemia cells. *Sci Rep*. 2016;6:34413.
- Dayem A, Hossain MK, Lee SB, et al. The role of reactive oxygen species (ROS) in the biological activities of metallic nanoparticles. *Int J Mol Sci*. 2017;18:120.
- Verma A, Uzun O, Hu Y, et al. Surface-structure-regulated cell-membrane penetration by monolayer-protected nanoparticles. *Nat Mater*. 2008;7:588-595.
- Alarifi S, Ali D, Alkahtani S. Nanoalumina induces apoptosis by impairing antioxidant enzyme systems in human hepatocarcinoma cells. *Int J Nanomedicine*. 2015;10(1):3751-3760.
- Alkahtane AA, Alarifi S, Al-Qahtani AA, Ali D, Alomar SY, Aleissia M. S, Alkahtani S. Cytotoxicity and genotoxicity of cypermethrin in hepatocarcinoma cells: a dose- and time-dependent study. *Dose Response*, vol. 16, no. 2, 2018:1559325818760880.
- Borenfreund E, Puerner JA. Toxicity determined in vitro by morphological alterations and neutral red absorption. *Toxicol Lett*. 1985;24:119-124.
- Almeer RS, Ali D, Alarifi S, Alkahtani S, Almansour M. Green platinum nanoparticles interaction with HEK293 cells: cellular toxicity, apoptosis, and genetic damage. *Dose-Response*. 2018;16:1559325818807382.
- Bradford MM. A rapid and sensitive method for the quantitation of microgram quantities of protein utilizing the principle of protein dye binding. *Anal Biochem*. 1976;72:248-254.
- Ellman GL. Tissue sulfhydryl groups. *Arch Biochem Biophys*. 1959;82:70-77.
- Ohkawa NO, Yagi K. Assay for lipid peroxidation in animal tissue by thiobarbituric acid reaction. *Anal Biochem*. 1979;95:351-358.
- Alarifi S, Ali H, Alkahtani S, Aleissa MS. Regulation of apoptosis through bcl-2/bax proteins expression and DNA damage by nano-sized gadolinium oxide. *Int J Nanomedicine*. 2017;12:4541-4551.
- Ali D, Nagpure N, Kumar S, Kumar R, Kushwaha B. Genotoxicity assessment of acute exposure of chlorpyrifos to freshwater fish *Channa punctatus* (Bloch) using micronucleus assay and alkaline single-cell gel electrophoresis. *Chemosphere*. 2008;71:1823-1831.
- Sandercock DA, Coe JE, Di Giminiani P, Edwards S. A Determination of stable reference genes for RT-qPCR expression data in mechanistic pain studies on pig dorsal root ganglia and spinal cord. *Res Vet Sci*. 2017;114:493-501.
- Nita M, Grzybowski A. The role of the reactive oxygen species and oxidative stress in the pathomechanism of the age-related ocular

- diseases and other pathologies of the anterior and posterior eye segments in adults. *Oxidative Medicine and Cellular Longevity*. 2016;2016:3164734.
25. Hirsch T, Marchetti P, Susin SA, et al. The apoptosis-necrosis paradox, apoptogenic proteases activated after mitochondrial permeability transition determine the mode of cell death. *Oncogene*. 1997;15:1573-1581.
26. Kim JS, Kuk E, Yu KN, Kim JH, Park SJ, Lee HJ. Antimicrobial effects of silver nanoparticles. *Nanomedicine*. 2007;3:95-101.
27. Krishnamoorthy S. *Nanomaterials: A Guide to Fabrication and Applications Technology & Engineering*. Boca Raton, Florida: CRC Press; 2015.
28. Petosa AR, Jaisi DP, Quevedo IR, Elimelech M, Tufenkji N. Aggregation and deposition of engineered nanomaterials in aquatic environments: role of physicochemical interactions. *Environ Sci Tech*. 2010;44:6532-6549.
29. Mironava T, Simon M, Rafailovich MH, Rigas B. Platinum folate nanoparticles toxicity: cancer vs. normal cells. *Toxicol in Vitro*. 2013;27:882-889.
30. Bendale Y, Bendale V, Paul S, Bhattacharyya SS. Green synthesis, characterization and anticancer potential of platinum nanoparticles. *Zhong Xi Yi Jie he Xue Bao*. 2012;10:681-689.
31. Gaetke LM, Chow CK. Copper toxicity, oxidative stress, and antioxidant nutrients. *Toxicology*. 2003;189(1-2):147-163.
32. Beckhauser TF, Francis-Oliveira J, Pasquale RD. Reactive oxygen species: physiological and physiopathological effects on synaptic plasticity. *J Exp Neurosci*. 2016;10(1):23-48.
33. Susin SA, Zamzami N, Kroemer G. Mitochondria as regulators of apoptosis: doubt no more. *Biochimica et Biophysica Acta (BBA) - Bioenergetics*. 1998;1366(1-2):151-165.
34. Yuan J, Murrell GAC, Trickett A, Wang MX. Involvement of cytochrome *c* release and caspase-3 activation in the oxidative stress-induced apoptosis in human tendon fibroblasts. *Biochimica et Biophysica Acta (BBA) - Molecular Cell Research*. 2003;1641(1):35-41. 20.
35. Greulich C, Diendorf J, Gessmann J, et al. Cell type-specific responses of peripheral blood mononuclear cells to silver nanoparticles. *Acta Biomater*. 2011;7:3505-3514.
36. Bahadar H, Maqbool F, Niaz K, Abdollah M. Toxicity of nanoparticles and an overview of current experimental models. *Iran Biomed J*. 2016;20(1):1-11.
37. Vanlangenakker N, Vanden BT, Krysko DV, Festjens N, Vandenabeele P. Molecular mechanisms and pathophysiology of necrotic cell death. *Curr Mol Med*. 2008;8:207-220.
38. Ghosh J, Das J, Manna P, Sil PC. Taurine prevents arsenic-induced cardiac oxidative stress and apoptotic damage: role of NF-kappa B, p38 and JNK MAPK pathway. *Toxicol Appl Pharmacol*. 2009;240:73-87.
39. Mattson MP, Keller JN, Begley JG. Evidence for synaptic apoptosis. *Exp Neurol*. 1998;153:35-48.

How to cite this article: Almarzoug MHA, Ali D, Alarifi S, Alkahtani S, Alhadheq AM. Platinum nanoparticles induced genotoxicity and apoptotic activity in human normal and cancer hepatic cells via oxidative stress-mediated Bax/Bcl-2 and caspase-3 expression. *Environmental Toxicology*. 2020; 1-12. <https://doi.org/10.1002/tox.22929>